

Intranuclear cascade model including collective excitations and trajectory deflections for $(p, p'x)$ reactions around 50 MeV

Yusuke Uozumi,^{*} Takahiro Yamada, and Sho Nogamine*Department of Applied Quantum Physics and Nuclear Engineering, Kyushu University, 744 Motoooka, Nishi-ku, Fukuoka 819-0395, Japan*

Masahiro Nakano

Junshin Gakuen University, 1-1-1 Chikushigaoka, Minami-ku, Fukuoka 815-8510, Japan

(Received 29 May 2012; published 18 September 2012)

Collective excitations and trajectory deflection are investigated to lower the applicable energy range of the intranuclear cascade model to around 50 MeV. First, inclusive $(p, p'x)$ reaction processes that lead to noncollective and collective excitations are formulated under the Born approximation. Then, collective excitations and trajectory deflection are introduced into the framework of the intranuclear cascade model. As collective excitations, low-energy vibrational excitations and giant resonances are considered. The trajectory deflection is assumed to be given by the experimental angular distribution of proton-nucleus elastic scattering. Finally, numerical calculations are conducted for $(p, p'x)$ reactions on ^{56}Fe at 29.9 and 61.5 MeV. The predictive capability of the proposed model is validated through comparison with experimental observations. The proposed model gives reasonably good predictions of $(p, p'x)$ reactions and proton elastic scatterings.

DOI: [10.1103/PhysRevC.86.034610](https://doi.org/10.1103/PhysRevC.86.034610)

PACS number(s): 24.10.Lx, 25.40.Fq

I. INTRODUCTION

The intranuclear cascade (INC) model [1,2] is among the most powerful tools for predicting the cross sections of nucleon-nucleus spallation reactions and plays an important role in transport code systems such as PHITS [3] and GEANT4 [4]. Over the years, many studies [5–12] have been devoted to improving the accuracy of the INC model. As a consequence, the INC model now has high predictive power at energies above a few hundred MeV. For broadening the applicability of transport codes, however, extension of the INC model to energies below 100 MeV is necessary. Since the exciton model [13,14] is used to calculate the inclusive spectra of nuclear reactions in this low-energy domain, an interesting avenue of research is to explore whether the INC model can be applied to account for these spectra. To this end, major modification of the INC model is necessary in order to include physical aspects neglected in previous studies.

The essential difference between low- and high-energy reactions should be the strength ratio of collective and noncollective excitations. Collective states populated in $(p, p'x)$ reactions are observed below excitation energies of 20 MeV. When the beam energy is 50 MeV or lower, observed spectra correspond to transitions involving collective excitation. Above 100 MeV, large portions of spectra correspond to noncollective excitations.

The INC model assumes that nuclear reactions can be described by sequential nucleon-nucleon (NN) collisions inside the nucleus and that all nucleons other than the colliding pair behave as spectators; this means that only noncollective states are considered in the model. This assumption leads to

poor predictive power at low beam energies. The inclusion of collective excitations should therefore be a key to extending the INC model to low energies. It bears emphasizing that all existing models (Feshback-Kerman-Koonin (FKK) [15], Tamura-Udagawa-Lenske (TUL) [16], Semi-Classical Distorted Wave (SCDW) [17,18], etc.) lack explicit treatment of collective excitations.

To extend the INC model, another key should be the influence of nuclear potential on particle trajectory. Although the INC model disregards particle deflection due to refraction and diffraction, these phenomena are more strongly evident in angular distributions with decreasing beam energies. Similarly, particle deflection due to nuclear potential should also be incorporated into the extended model.

The applicability of INC at energies below 100 MeV has been investigated elsewhere. Cugnon and Henrotte [9] proposed the Intranuclear cascade Liège (INCL) model and investigated its performance. Duarte [10] included nuclear potential in the BRIC model to account for particle deflection. In that model, particle trajectories are given by the classical mechanics of a particle in a potential. This prescription is insufficient to reproduce large-angle scattering, which is ascribable to the diffraction of waves. Both Cugnon and Duarte disregarded the contribution of collective excitations.

In the present study, we expand the INC framework by including collective excitations and trajectory deflections. The paper is organized as follows. In Sec. II, we discuss possible excited states populated by nuclear reactions below 100 MeV. Although all theoretical models of inclusive reactions consider only particle-hole excitations, we aim to demonstrate the importance of collective excitations. Formulations of one-step double-differential cross sections (DDXs) are deduced on the basis of the distorted wave Born approximation (DWBA). Here, we restrict ourselves to $(p, p'x)$ reactions. In Sec. III, our model is further simplified to fit within the INC

^{*} uozumi@nucl.kyushu-u.ac.jp

framework. Optimal parameters are determined for collective excitations and deflections. In Sec. IV, DDXs of $^{56}\text{Fe}(p, p'x)$ reactions at 29.9 and 61.5 MeV are calculated and compared with experimental observations to validate the proposed model.

II. FORMULATION OF ONE-STEP DOUBLE-DIFFERENTIAL CROSS SECTIONS

Let us consider nucleon-induced nucleon-emitting reactions where the target nucleus is excited to any state along a continuum. To examine the reaction processes missed under the conventional INC model, we deduce the first-order DWBA form for the possible excitations in inclusive $(p, p'x)$ reactions at several tens of MeV.

Most previous theoretical models of inclusive reactions consider only the simplest ground state of the target nucleus, in which all nucleons follow the independent-particle motion. These models assume excited states are only particle-hole states. In actuality, however, there are also collective excitation states.

Tamura *et al.* [16] assumed that the excited states $|\Phi_n\rangle$ include 1p-1h states and other more complicated states. The states are expressed as

$$|\Phi_n\rangle = \sum_B a_B |\Phi_B\rangle + \delta |\Phi_n\rangle. \quad (1)$$

The one-step process excites the $|\Phi_B\rangle$ state only, and two or more steps may excite the $\delta |\Phi_n\rangle$ state. We make the further assumption that the 1p-1h states are decomposed into noncollective states $|\Phi_{B1}\rangle$ and collective states $|\Phi_{B2}\rangle$:

$$\sum_B a_B |\Phi_B\rangle = \sum_{B1} a_{B1} |\Phi_{B1}\rangle + \sum_{B2} a_{B2} |\Phi_{B2}\rangle. \quad (2)$$

The noncollective state is expressed as

$$|\Phi_{B1}\rangle = (|\phi_{1p}\rangle |\Phi_{1h}\rangle)_{B1}, \quad (3)$$

where

$$|\Phi_{1h}\rangle \equiv c |\Phi_0\rangle.$$

The collective state is expressed as

$$|\Phi_{B2}\rangle = |\Phi_{\text{coll},\lambda}\rangle, \quad (4)$$

where λ represents the quantum number of the state. In the case of a vibrational state, it can be written by using the boson creation operator:

$$|\Phi_{\text{coll},\lambda}\rangle = b_\lambda^\dagger |\Phi_0\rangle. \quad (5)$$

Following Tamura *et al.*, we express the amplitude of the one-step DWBA transition to the excited state $|\Phi_{B1}\rangle$ as follows:

$$T_{nB1}^{(1)} = \langle x_b | \langle \Phi_{B1} | v | \Phi_0 \rangle | x_a \rangle = \sum_B a_{B1} t_{ba}^{B1}, \quad (6)$$

where

$$t_{ba}^{B1} = \langle x_b | v_{B10} | x_a \rangle; \\ v_{B10} = \langle \Phi_{B1} | v | \Phi_0 \rangle.$$

The DDX for the one-step process is given by

$$\frac{\partial^2 \sigma_{B1}^{(1)}}{\partial \Omega \partial \omega} = \frac{\mu^2}{(2\pi \hbar^2)^2} \frac{k_f}{ki} |T_{nB1}^{(1)}|^2 \delta(E_n - E_x), \quad (7)$$

where E_n is the eigenenergy of $\delta |\Phi_n\rangle$ and E_x is the excitation energy, which satisfies the relation $E_x = E_{\text{in}} - E_{\text{exit}}$, where E_{in} and E_{exit} are proton kinetic energies of incident and exit channels, respectively.

In the same way, DDX of the transition to $\delta |\Phi_{B2}\rangle$ state is

$$\frac{\partial^2 \sigma_{B2}^{(1)}}{\partial \Omega \partial \omega} = \frac{\mu^2}{(2\pi \hbar^2)^2} \frac{k_f}{ki} |T_{nB2}^{(1)}|^2 \delta(E_n - E_x) \quad (8)$$

with the transition amplitude

$$T_{nB2}^{(1)} = \langle x_b | \langle \Phi_{B2} | v | \Phi_0 \rangle | x_a \rangle = \sum_B a_{B2} t_{ba}^{B2}, \quad (9) \\ t_{ba}^{B2} = \langle x_b | v_{B20} | x_a \rangle; \quad v_{B20} = \langle \Phi_{B2} | v | \Phi_0 \rangle.$$

The DDX of the one-step transition to states of excitation energy E_x is expressed by

$$\frac{\partial^2 \sigma^{(1)}}{\partial \Omega \partial \omega} \Big|_{E_x} = \frac{\mu^2}{(2\pi \hbar^2)^2} \frac{k_f}{ki} |T_{nB}^{(1)}|^2 \delta(E_n - E_x) \\ = \frac{\partial^2 \sigma_{B1}}{\partial \Omega \partial \omega} \Big|_{E_x} + \frac{\partial^2 \sigma_{B2}}{\partial \Omega \partial \omega} \Big|_{E_x}. \quad (10)$$

Here we disregard the interference between the two terms on the right-hand side of Eq. (10), since we cannot calculate the cross term. The collective states are mixtures of particle-hole states. The collective states are populated through small momentum transfers, and consequently, most of the transitions are missed in INC because of its insufficient treatment of Pauli blocking. This point is discussed again in Sec. IV. The INC model is assumed to include only $|\Phi_{B1}\rangle$ as the final state, but excludes most of $|\Phi_{B2}\rangle$. Excitation to $|\Phi_{B1}\rangle$ is nearly equivalent to the one-step INC calculation, and hence we obtain the following relations:

$$\frac{\partial^2 \sigma_{B1}^{(1)}}{\partial \Omega \partial \omega} \cong \frac{\partial^2 \sigma_{\text{INC}}^{(1)}}{\partial \Omega \partial \omega}. \quad (11)$$

III. DOUBLE-DIFFERENTIAL CROSS SECTION CALCULATION

A. Formulation and derivation

To calculate DDX spectra of inclusive reactions, Eq. (10) must be extended to a nonperturbative form. Also, reasonably short computation time is essential for practical applications. Note that we aim to construct a model that has reasonable good predictive power for energy and angular distributions over a wide range of energy transfers and mass numbers of target nuclei, rather than a model that has high predictive power for a specific transition. Accordingly, we further simplify Eq. (10) to fit within the INC framework and deduce the reaction rate of inclusive $(p, p'x)$ reactions in a form that can be calculated by the Monte Carlo method. The spin and isospin degrees of

freedom are ignored for the sake of clarity and simplicity in the following discussion.

Excitations to noncollective states are ascribable to local NN collisions in a nucleus, because they are accompanied by large energy transfers and the surrounding nucleons behave as spectators. The probability of the process in which one of the colliding particles is scattered to angle θ and energy ε is given by

$$P_{nc}(\theta, \varepsilon) = Q \frac{\rho(\mathbf{r}) \Delta r^3}{A} \frac{1}{\sigma_{NN}} \left(\int_{p < p_F} \frac{\partial \sigma_{NN}}{\partial \Omega} dp \right)_\theta \times \delta(E_{in} - \varepsilon - E_{xnc}), \quad (12)$$

where σ_{NN} is the NN collision cross section, ρ is the local density of nucleons at the collision point where the NN collision occurs, and A is the mass number of the target nucleus. The projection operator Q for Pauli blocking is

$$Q|ij\rangle = \begin{cases} |ij\rangle & \text{if both particles } i \text{ and } j \\ & \text{are above the Fermi surface,} \\ 0 & \text{otherwise.} \end{cases}$$

With this probability, the DDX of noncollective excitation is written as

$$\frac{\partial^2 \sigma_{B1}^{(1)}}{\partial \Omega \partial \omega} = \sigma_{total} P_{def}^{\varepsilon';in}(\theta_{in}) P_{nc}(\theta_{nc}, \varepsilon) P_{def}^{\varepsilon;ex}(\theta_{ex}), \quad (13)$$

where σ_{total} is the total cross section of nucleon-nucleus interactions including elastic scattering and $P_{def}^\varepsilon(\theta)$ is the probability of deflection by angle θ due to the nuclear potential at the incident and exit channels of a proton with energy of ε . We assume $P_{def}^\varepsilon(\theta)$ is roughly given by the angular distribution of proton-nucleus elastic scattering:

$$P_{def}^\varepsilon(\theta) = \frac{1}{\sigma_{el}^\varepsilon} \frac{d\sigma_{el}^\varepsilon}{d\Omega}(\theta), \quad (14)$$

and

$$\sigma_{el}^\varepsilon = \int \frac{d\sigma_{el}^\varepsilon(\theta)}{d\Omega} d\Omega.$$

The deflection is assumed to occur at the nuclear surface when the particle enters and leaves the nucleus and is treated as a proton-nucleus interaction, not an intranuclear NN interactions. Since nucleon spin is ignored, the azimuth angles of every scattering are assumed to be isotropic.

The probability of a collective excitation process cannot be written in the same manner as Eq. (12), because the energy transfer is smaller than the nucleon binding energy and both the struck nucleon and all other nucleons are influenced strongly by the collision. We assume that the process can be regarded as an interaction between the incident nucleon and the target nucleus and takes place at the nuclear surface. We also assume that the deflection during the interaction is negligibly small. Although the angular distribution is sensitive to momentum transfer, a highly precise distribution is not necessary for our purposes. Then we obtain the following relations:

$$\frac{\partial^2 \sigma_{B2}^{(1)}}{\partial \Omega \partial \omega} = \sigma_{total} P_{def}^{\varepsilon';in}(\theta_{in}) P_{co}(\varepsilon) P_{def}^{\varepsilon;ex}(\theta_{ex}), \quad (15)$$

and

$$P_{co}(\varepsilon) = \frac{1}{\sigma_{total}} \frac{d\sigma_{co}}{d\omega} \delta(E_{in} - \varepsilon - E_{xco}), \quad (16)$$

where $\frac{d\sigma_{co}}{d\omega}$ is the energy-differential cross sections for collective excitations.

By using Eqs. (12), (14), and (16), we define the probability of a one-step (p, p') reaction. Let us first define the time order as

$$0 < t_1 < t_2 < t_3 < \dots < t_m < t_M < \infty.$$

The projectile touches the nuclear surface at time t_1 , and the cascade process finishes at t_M . Next, we introduce the operator for space development:

$$\Gamma(r, r') : \mathbf{r} \rightarrow \mathbf{r}' = \mathbf{r} + \mathbf{v}t, \quad (17)$$

$$\forall t > 0, \quad r' < R_{max}, \quad p > p_F,$$

where \mathbf{v} is the velocity of particles inside the nucleus and R_{max} is the maximum radius of the nucleus. Thus the one-step reaction probability is given by

$$P^{(1)}(\theta, \varepsilon) = P_{def}^{\varepsilon';in}(\theta_{in}, t_1) \Gamma P_{co}(\varepsilon, t_2) \Gamma P_{def}^{\varepsilon;ex}(\theta_{ex}, t_4) + P_{def}^{\varepsilon';in}(\theta_{in}, t'_1) \Gamma P_{nc}(\theta_{nc}, \varepsilon, t'_2) \Gamma P_{def}^{\varepsilon;ex}(\theta_{ex}, t'_4). \quad (18)$$

The corresponding expression of the conventional INC is written in the following form:

$$P_{INC}^{(1)}(\theta, \varepsilon) = \Gamma P_{nc}(\theta, \varepsilon, t) \Gamma. \quad (19)$$

The formulation for the two-step process can be easily obtained from Eq. (19). Note that noncollective excitation involves a large momentum transfer and can occur more than twice sequentially. In contrast, collective excitation is critically sensitive to the nucleus type and occurs once. However, collective excitation may be accompanied by a subsequent noncollective excitation process. Two two-step reaction paths are assumed: One induces noncollective excitations twice; in the other, collective excitation is followed by noncollective excitation. These reaction pathways are expressed as

$$P^{(2)}(\theta, \varepsilon) = P_{def}^{\varepsilon';in}(\theta_{in}, t_1) \Gamma P_{nc}(\theta_{nc1}, \varepsilon_{nc1}, t_2) \Gamma P_{nc}(\theta_{nc2}, \varepsilon_{nc2}, t_3) \times \Gamma P_{def}^{\varepsilon;ex}(\theta_{ex}, t_4) \quad (20)$$

and

$$P^{(2)}(\theta, \varepsilon) = P_{def}^{\varepsilon';in}(\theta_{in}, t_1) \Gamma P_{co}(\theta_{co}, \varepsilon_{co}, t_2) \Gamma P_{nc}(\theta_{nc}, \varepsilon_{nc}, t_3) \times \Gamma P_{def}^{\varepsilon;ex}(\theta_{ex}, t_4), \quad (21)$$

respectively.

Note that Eq. (20) is very similar in form to Eq. (3.19) of Kawai and Weidenmuller [18]. Their intuitive explanation also applies to our Eq. (20). In particular, they concluded that the propagator is expressed by the geometrical factor and the attenuation factor. This is consistent with our classical treatment.

Finally, we deduce the reaction probability in a nonperturbative form:

$$P^{np}(\theta, \varepsilon) = P_{def}^{\varepsilon';in}(\theta_{in}, t_1) [1 + P_{co}(\theta_{co}, \varepsilon_{co}, t_2)] \times G_{cas}(\theta_{cas}, \varepsilon_{cas}) P_{def}^{\varepsilon;ex}(\theta_{ex}, t_{m+1}) \quad (22)$$

for

$$G_{\text{cas}}(\theta, \varepsilon) = \Gamma + \Gamma P_{\text{nc}}(\theta_{m1}, \varepsilon_{m1}, t_{m1})\Gamma + \Gamma P_{\text{nc}}(\theta_{m2}, \varepsilon_{m2}, t_{m2}) \\ \times \Gamma P_{\text{nc}}(\theta_{m3}, \varepsilon_{m3}, t_{m3})\Gamma + \dots$$

The DDX is given by

$$\frac{\partial^2 \sigma}{\partial \varepsilon_f \partial \Omega_f} = \sigma_{\text{total}} \frac{1}{2\pi \Delta E \Delta \cos(\theta)} \sum_k P^k(\theta, \varepsilon), \quad (23)$$

where ΔE and $\Delta \cos \theta$ are the bin widths of the outgoing energy ε and emission angle θ , respectively.

We note that Eq. (22) includes the expression for elastic scattering:

$$P(\theta, \varepsilon) = P_{\text{def}}^{\varepsilon;\text{in}}(\theta_{\text{in}}, t_1)\Gamma P_{\text{def}}^{\varepsilon;\text{ex}}(\theta_{\text{Ref.}}, t_2). \quad (24)$$

However, this is only the deflection of the particle trajectory. Two-body kinematics does not hold. The deviation from the energy conservation law is very small in many cases, so we may neglect this problem.

B. Outline of INC model

The present study was carried out by extending the INC model code investigated in Ref. [11], where details of the model were described. Here the main features are only briefly presented. For the target nucleus, initial nucleon positions are randomly distributed inside a sphere, in which nucleon density follows the Woods-Saxon distribution for a nuclear radius r_0 of $(0.976 + 0.0206A^{1/3})^{1/3}A^{1/3}$ fm (where A is the nuclear mass number) and a diffuseness a_0 of 0.54 fm. The maximum nuclear radius is defined as $R_{\text{max}} = r_0 + 4a_0$, and the total cross section is given by

$$\sigma_{\text{total}} = \pi R_{\text{max}}^2.$$

All the nucleons are inside a binding potential V_0 of -45 MeV. The initial nucleon momenta are uniformly distributed inside the Fermi sphere. Next, a projectile is sent to the target nucleus with an impact parameter chosen at random. Intranuclear NN collisions are described by the cross section σ_{NN} . When an energetic particle approaches another target nucleon to within a distance of $\sqrt{\sigma_{NN}/\pi}$, they undergo a collision. The Pauli blocking operator Q is introduced as

$$Q = 1 - [1 - \Theta(p_j - p_F)], \quad (25)$$

where p_i and p_j are the momenta of the scattered particles, p_F is the Fermi momentum, and Θ denotes the Heaviside function. The parameters of the NN cross sections and angular distributions are taken from the treatment presented in Ref. [19].

The high predictive power of this INC model has been verified in Ref. [11] in terms of $(p, p'x)$ reactions on many target nuclei at bombarding energies of 300 and 392 MeV. In Ref. [20], reasonable agreement was also found with experimental (p, nx) reaction data at 120 and 160 MeV. Since the physical models and parameter values involved in this INC are barely sensitive to the bombarding energy, we use the same models and parameter values in this work.

The static phase of nuclear reactions is computed by the generalized evaporation model (GEM) code [21]. At the end

of each INC calculation, information about residual nuclei is transferred to the evaporation stage of GEM. The input configuration of the residue for GEM is characterized by the number of protons and neutrons, the nuclear excitation energy, and the momentum.

C. Parameterization

1. Probability of deflection angle

Since angular distributions of elastic scattering are used to express the particle deflection in inclusive reactions, their interference structures are not important. We introduced a model to describe the probability of angular distributions of elastic scattering in our previous work [22]. Presently, we simplify that model by disregarding the Coulomb term:

$$P_{\text{def}}^{\varepsilon}(\theta; A) = \exp[-0.001(1.3\varepsilon + 6 \ln A - 5)\theta]. \quad (26)$$

Typical examples are shown in Figs. 1 and 2, which present comparisons between calculations and experimental results for proton elastic scattering of ^{56}Fe at 39.8 MeV [23] and 65 MeV [24], respectively. Magnitudes of calculated values are scaled to the level of the experimental values. Although rather large discrepancies are observed at forward angles, the sharp rise observed in experiments due to the Coulomb repulsion force is beyond the scope of this model. General trends in the angular distributions are reproduced reasonably well by the present model.

2. Collective excitations

There are two types of collective excitations: One is the low-energy excitation due to rotational and vibrational modes; the other is the high-energy excitation of giant resonances. In

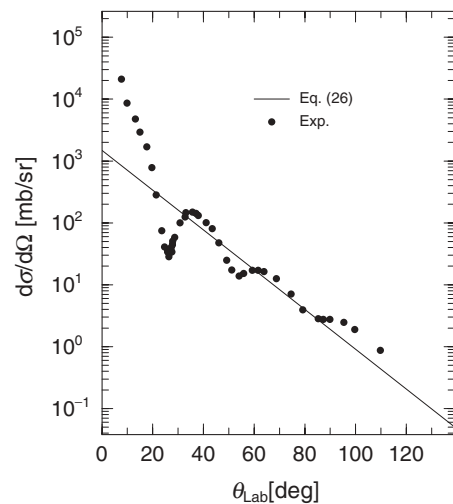


FIG. 1. Comparison of experiment and systematic calculation with Eq. (26) for proton elastic scattering on ^{56}Fe at 39.8 MeV. Experimental data are taken from Ref. [23]. Calculation results are scaled to experimental values.

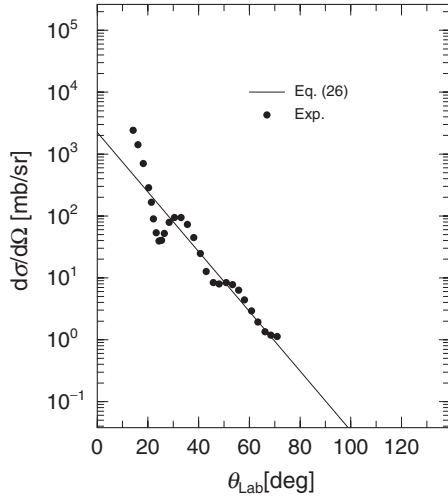


FIG. 2. Same as Fig. 1, but for 65 MeV. Experimental data are taken from Ref. [24].

the case of (p, p') reactions, the giant quadrupole resonance (GQR) has the greatest strength. We assume that $\frac{d\sigma_{co}}{d\omega}$ is given by the incoherent sum of energy-differential cross sections for these two excitations:

$$\frac{d\sigma_{co}}{d\omega} = \frac{d\sigma_{GQR}}{d\omega} + \frac{d\sigma_{LE}}{d\omega}. \quad (27)$$

By using the Breit-Wigner distribution, the first term is expressed as

$$\frac{d\sigma_{GQR}}{d\omega}(E_x) = \sigma_{GQR} \frac{1}{\pi} \frac{\Gamma_{GQR}/2}{(E_{GQR} - E_x)^2 + (\Gamma_{GQR}/2)^2}, \quad (28)$$

where E_{GQR} is the average excitation energy of the resonance and Γ_{GQR} is the resonance width. In the present calculation, we used $\Gamma_{GQR} = 8$ (MeV) and $E_{GQR} = 65A^{-1/3}$ (MeV). We determined that $\sigma_{GQR} = 0.065\sigma_{total}$ best reproduces the experimental DDX spectra.

Low-energy collective excitations are well accounted for by DWBA. In the case of the $^{56}\text{Fe}(p, p')$ reaction, main transition strengths were measured experimentally and their

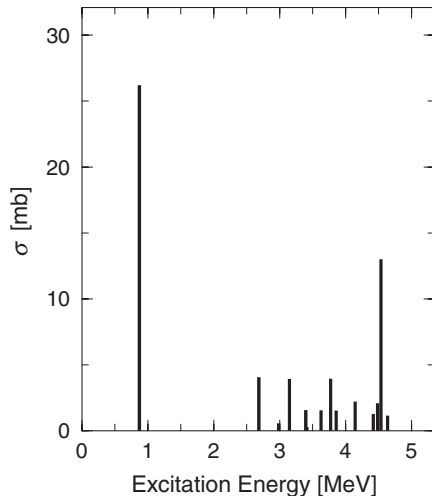


FIG. 3. Strength function of the $^{56}\text{Fe}(p, p')$ reaction at 65 MeV.

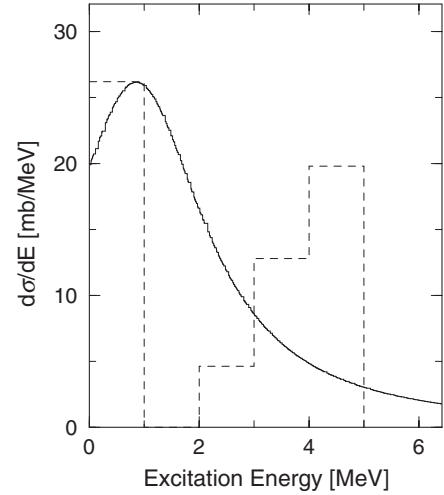


FIG. 4. Broken histogram is the strength density distribution of the $^{56}\text{Fe}(p, p')$ reaction at 65 MeV. Solid curve is the distribution approximated by the Breit-Wigner function.

deformation parameters have been determined and listed in the Evaluated Nuclear Structure Data File (ENSDF) database [25]. The strength function, which was calculated with the CCONE code [26], is shown in Fig. 3 for the $^{56}\text{Fe}(p, p')$ reaction at 65 MeV. We express the strength function by using the density distribution in the same way as for GQR. First, the strength function was replaced by the strength density indicated by the broken-line histogram in Fig. 4. Then the Breit-Wigner curve was determined as shown by the solid line.

$$\frac{d\sigma_{LE}}{d\omega}(E_x) = \sigma_{LE} \frac{1}{\pi} \frac{\Gamma_{LE}/2}{(E_{LE} - E_x)^2 + (\Gamma_{LE}/2)^2}, \quad (29)$$

where $\sigma_{LE} = 0.28$ (mb), $\Gamma_{LE} = 3$ (MeV), and $E_{LE} = 0.846$ (MeV). The σ_{LE} value corresponds to the one-step reaction given by the first term on the right-hand side of

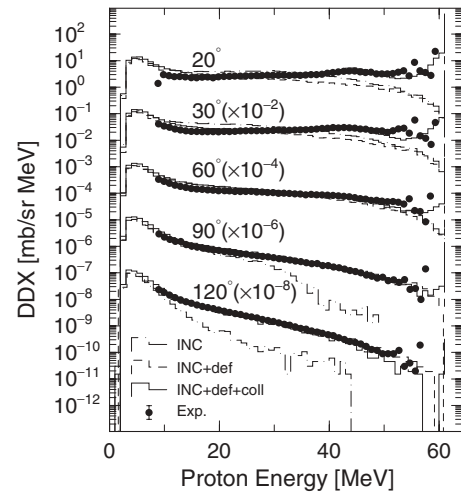


FIG. 5. Comparison of spectral DDXs of the $^{56}\text{Fe}(p, p')$ reaction at 61.5 MeV between experiment and calculations under three different conditions. Factors in parentheses are multipliers to avoid pile up.

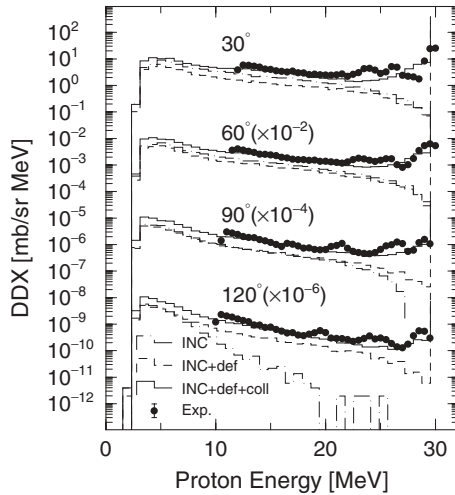


FIG. 6. Same as Fig. 5, but for beam energy of 29.9 MeV.

Eq. (19). Taking a multistep process such as Eq. (21) into account, we arrived at the value of $\sigma_{LE} = 0.54$ (mb).

IV. CALCULATION RESULTS AND DISCUSSION

To validate the present model, DDX spectra were calculated for $^{56}\text{Fe}(p, p')$ reactions at 29.9 and 61.5 MeV and compared with experimental observations. Spectral DDXs for 61.5 MeV are shown in Fig. 5 from 20° to 120° . In order to avoid overlap, factors indicated in the figure are multiplied. Closed circles indicate experimental data taken from Ref. [27]. The numerical data were taken from the database EXFOR [28], which excludes elastic scattering data. Let us first examine the influence of trajectory deflection. Broken lines and dash-dotted lines show the results for INC with and without deflection, respectively. The influence of deflection is especially strong at 90° and 120° ; the considerable underestimation is improved upon, and close agreement between calculation and experiment is obtained. In addition, overestimations between 10 and

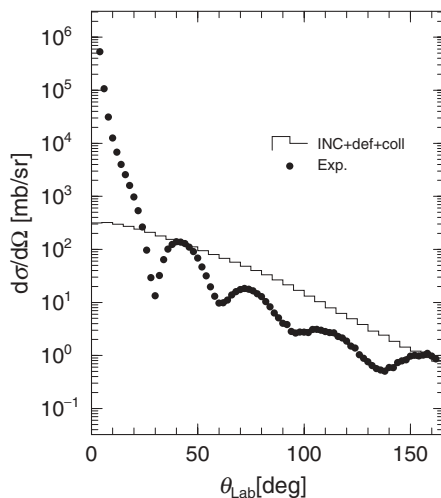
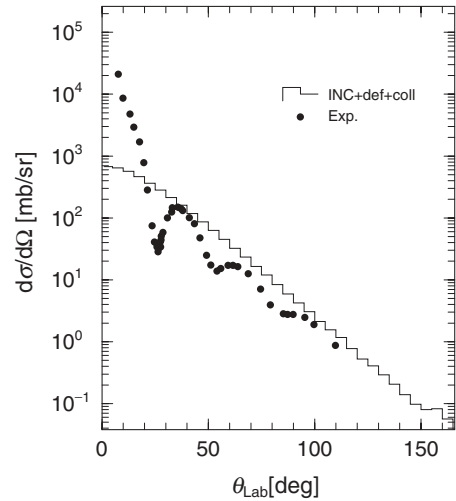

 FIG. 7. Comparison of angular distribution of proton elastic scattering on ^{56}Fe at 30.3 MeV between experiment and calculation.


FIG. 8. Same as Fig. 7, but for beam energy of 39.8 MeV.

30 MeV at 30° are resolved. However, discrepancies remain in the highest energy part of spectra at 20° and 30° . Next, we investigate the contribution from collective excitations. The solid and broken lines respectively indicate the results of calculations with and without collective excitations. Both include particle deflection. Compared with experiments, calculations without collective excitations give smaller DDXs for transitions accompanying small momentum transfers. As discussed in Sec. II, this underestimation may be attributable to the crude treatment of Pauli blocking in Eq. (25). However, the question remains as to whether the present method would expand the Hilbert space. The inclusion of collective excitations appears to improve the calculation accuracy and results in close agreement with experimental observations.

Further validation is done for 29.9 MeV (Fig. 6) in the same manner as for 61.5 MeV. Experimental DDX data for the $^{56}\text{Fe}(p, p')$ reaction are taken from Ref. [29]. From comparison between dash-dotted lines and broken lines, the inclusion of particle deflection is found to improve upon the underestimation found under the existing model. In particular,

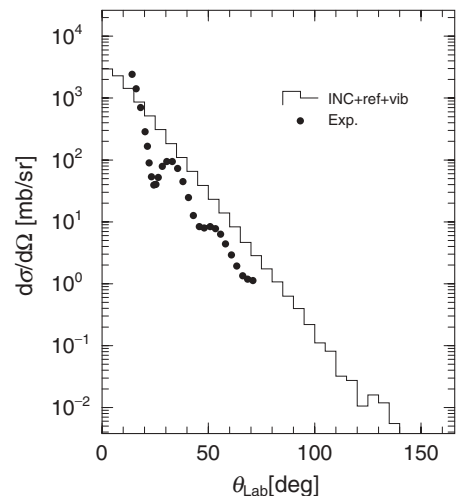


FIG. 9. Same as Fig. 7, but for beam energy of 65 MeV.

the influence of deflection is appreciable at 120° . Nevertheless, slight underestimation remains at all angles over the entire energy range. Solid lines show the results of calculations including both deflection and collective excitation. It is found that, overall, close agreement is achieved. Although a slight discrepancy arises from the small structures in experimental spectra in the low excitation energy regime, which are attributed to discrete level populations. Here our aim is to reproduce the general trend of energy distributions, and these structures are beyond the scope of this paper.

Phenomena like elastic scattering are observed at the highest energies of the calculation results in Figs. 5 and 6. These protons experienced no energy loss, but are deflected twice at the entrance and exit channels. This process corresponds to the term given by Eq. (24). Comparisons with experimental elastic scattering angular distributions were carried out on ^{56}Fe for 30.3, 39.8, and 65 MeV in Figs. 7 to 9, respectively, since no data are available at energies 29.9 and 61.5 MeV. Closed circles

indicate experimental data taken from Refs. [30] and [23,24]. Calculation results are indicated by solid lines. All of these figures show that not only the trend of angular distributions but also their magnitudes are roughly reproduced in the present calculation. Large-angle scattering, which cannot be accounted for by classical particle dynamics, is reproduced.

V. CONCLUSION

To widen the applicable range of the INC model to the low energy regime below 100 MeV, we introduced collective excitation and trajectory deflection for both projectiles and ejectiles. The calculation results for inclusive $^{56}\text{Fe}(p, p'x)$ reactions at 29.9 and 61.5 MeV indicate that the proposed model has high predictive power. Close agreement was obtained for the entire range of experimental observations of proton- ^{56}Fe elastic scattering at 30.3, 39.8, and 65 MeV.

-
- [1] M. Goldberger, *J. Phys. Rev.* **74**, 1269 (1948).
 [2] N. Metropolis, *J. Phys. Rev.* **110**, 185 (1958), and references therein.
 [3] K. Niita, N. Matsuda, Y. Iwamoto, H. Iwase, T. Sato, H. Nakashima, Y. Sakamoto, and L. Sihver, *JAEA-Data/Code* 2010-022, 1 (2010).
 [4] J. Allison *et al.*, *IEEE Trans. Nucl. Sci.* **53**, 270 (2006).
 [5] H. W. Bertini, *J. Phys. Rev.* **188**, 1711 (1969).
 [6] Y. Yariv and Z. Fraenkel, *Phys. Rev. C* **20**, 2227 (1979).
 [7] S. G. Mashnik, *Nucl. Phys. A* **568**, 703 (1994).
 [8] J. Cugnon, C. Volant, and S. Vuillier, *Nucl. Phys. A* **620**, 475 (1997).
 [9] J. Cugnon and P. Henrotte, *Eur. Phys. J. A* **16**, 393 (2003).
 [10] H. Duarte, *Phys. Rev. C* **75**, 024611 (2007).
 [11] H. Iwamoto, M. Imamura, Y. Koba, Y. Fukui, G. Wakabayashi, Y. Uozumi, T. Kin, Y. Iwamoto, S. Hohara, and M. Nakano, *Phys. Rev. C* **82**, 034604 (2010).
 [12] Y. Uozumi, Y. Sawada, A. Mzhavia, S. Nogamine, H. Iwamoto, T. Kin, S. Hohara, G. Wakabayashi, and M. Nakano, *Phys. Rev. C* **84**, 064617 (2011).
 [13] J. J. Griffin, *Phys. Rev. Lett.* **17**, 478 (1966); *Phys. Lett. B* **24**, 1967 (1967).
 [14] M. Blann, *Phys. Rev. Lett.* **27**, 337 (1971).
 [15] H. Feshbach, *Ann. Phys. (NY)* **125**, 429 (1980).
 [16] T. Tamura, T. Udagawa, and H. Lenske, *Phys. Rev. C* **26**, 379 (1982).
 [17] Y. L. Luo and M. Kawai, *Phys. Rev. C* **43**, 2367 (1991).
 [18] M. Kawai and H. A. Weidenmüller, *Phys. Rev. C* **45**, 1856 (1992).
 [19] J. Cugnon, D. D'Hote, and J. Vandermeulen, *Nucl. Inst. Meth. B* **111**, 215 (1996).
 [20] H. Iwamoto, M. Imamura, N. Koba, H. Fukuda, G. Wakabayashi, Y. Uozumi, and M. Nakano, in *Proceedings of the International Conference on Nuclear Data for Science and Technology, ND2007*, Vol. 2 (EDP sciences, France, 2008), p. 1147.
 [21] S. Furihata and T. Nakamura, *J. Nucl. Sci. Tech. Suppl.* **2**, 758 (2002).
 [22] H. Yoshida *et al.*, *Nucl. Inst. Meth. A* **411**, 46 (1998).
 [23] M. K. Brussel and J. H. Williams, *Phys. Rev.* **114**, 525 (1959).
 [24] R. DeLeo *et al.*, *Phys. Rev. C* **53**, 2718 (1996).
 [25] Evaluated Nuclear Structure Data File, <http://www.nndc.bnl.gov/ensdf/>.
 [26] O. Iwamoto, *J. Nucl. Sci. Technol.* **44**, 687 (2007).
 [27] F. E. Bertrand and R. W. Peele, *Phys. Rev. C* **8**, 1045 (1973).
 [28] EXFOR/CISISRS Experimental Nuclear Reaction Data, <http://www.nndc.bnl.gov/exfor/exfor00.htm>.
 [29] A. Duisebayev, K. M. Ismailov, and I. Boztosun, *Phys. Rev. C* **72**, 054604 (2005).
 [30] B. W. Ridley and J. F. Turner, *Nucl. Phys.* **58**, 497 (1964).